

See discussions, stats, and author profiles for this publication at: <https://www.researchgate.net/publication/323854484>

Performance and mechanism of simultaneous removal of Cd(II) and Congo red from aqueous solution by hierarchical vaterite spherulites

Article in Applied Surface Science · March 2018

DOI: 10.1016/j.apsusc.2018.03.081

CITATIONS

0

READS

77

6 authors, including:



Yuanyuan Chen

University of Science and Technology of China

2 PUBLICATIONS **0** CITATIONS

[SEE PROFILE](#)



Sheng-Hui Yu

Shaanxi University of Science and Technology

9 PUBLICATIONS **23** CITATIONS

[SEE PROFILE](#)



Gen-Tao Zhou

University of Science and Technology of China

70 PUBLICATIONS **1,132** CITATIONS

[SEE PROFILE](#)

Some of the authors of this publication are also working on these related projects:



heavy metals treatment [View project](#)



Full Length Article

Performance and mechanism of simultaneous removal of Cd(II) and Congo red from aqueous solution by hierarchical vaterite spherulites

Yuan-Yuan Chen^a, Sheng-Hui Yu^a, Hao-Fan Jiang^a, Qi-Zhi Yao^{b,*}, Sheng-Quan Fu^c, Gen-Tao Zhou^{a,*}^a CAS Key Laboratory of Crust-Mantle Materials and Environments, School of Earth and Space Sciences, University of Science and Technology of China, Hefei 230026, PR China^b School of Chemistry and Materials Science, University of Science and Technology of China, Hefei 230026, PR China^c Hefei National Laboratory for Physical Sciences at Microscale, University of Science and Technology of China, Hefei 230026, PR China

ARTICLE INFO

Article history:

Received 29 August 2017

Revised 26 February 2018

Accepted 10 March 2018

Available online 12 March 2018

Keywords:

Vaterite spherulites

Cd(II) ion

Congo red

Simultaneous removal

Removal mechanism

ABSTRACT

Hierarchical vaterite spherulites, synthesized by a simple injection-precipitation method at room temperature, were applied for the simultaneous removal of heavy metal Cd(II) and dye Congo red (CR) from aqueous solution. Batch experiments reveal that the maximum removal capacities of as-prepared vaterite spherulites to Cd(II) and CR are 984.5 and 89.0 mg/g, respectively, showing excellent removal performance for Cd(II) and CR. Furthermore, in the binary Cd(II)-CR system, the removal capacity of vaterite to Cd(II) is significantly enhanced at lower CR concentration (<100 mg/L), but inhibited at higher CR concentration (>100 mg/L). In contrast, the concurrent Cd(II) shows negligible effect on the CR removal. The simultaneous removal mechanism was investigated by FESEM, EDX, XRD, FT-IR and XPS techniques. The simultaneous removal of Cd(II) and CR in the binary system is shown to be a multistep process, involving the preferential adsorption of dye CR, stabilization of CR to vaterite, coordination of the adsorbed CR molecules with Cd(II), and transformation of vaterite into otavite. Given the facile and green synthesis procedure, and effective removal of Cd(II) and CR in the binary system, the obtained vaterite spherulites have considerable practical interest in integrative treatment of wastewater contaminated by heavy metals and dyes.

© 2018 Elsevier B.V. All rights reserved.

1. Introduction

Recently, combined pollution has been an increasingly hot topic in environmental studies. In particular, heavy metals and dyes often coexist in the effluents of textile, leather, cosmetic and papermaking industries because of the wide application of heavy metals (e.g., cadmium, copper and aluminum) in the dyeing process as mordant [1–3]. Both heavy metals and dyes could cause serious damages to human health due to their strong toxicity, environmental persistence and bioaccumulation [4,5]. For example, cadmium is a common hypertoxic contaminant [6]. Cadmium exposure can cause many diseases, such as emphysema, hypertension, diabetes mellitus and skeletal malformation due to the lack of homeostatic control for cadmium in the human body [7]. Congo Red (CR), one of the most widely used anionic disazo dyes, can be metabolized to cancerigenic benzidine in aquatic environment [8,9]. Currently, numerous conventional techniques are mainly focused on the removal of a single class of contaminants

(either heavy metals or dyes) [10–13]. However, the different physicochemical properties of heavy metals and dyes make the treatment of wastewater more challenging [14]. Growing evidence also suggested that the combined toxicities of heavy metal ions and dyes are generally larger than the simple adduct of their individual toxicity [15,16]. Therefore, developing facile and environmentally benign materials to simultaneously remove heavy metals and dyes from wastewater is urgent and crucial.

Calcium carbonate, occurring geologically as one of the main mineral constituents of sedimentary rocks and biologically as inorganic components in the skeletons of many mineralizing organisms [17,18], is one of the most abundant minerals in nature. It exists in three anhydrous crystal polymorphs: rhombohedral calcite, orthorhombic aragonite, and hexagonal vaterite [19]. Among them, calcite is the stable form under ambient conditions, aragonite is the high-pressure polymorph, while vaterite is thermodynamically unstable [20]. Calcium carbonate has important industrial applications in the areas of plastics, rubbers, papermaking, biomedical implant and drug delivery [21,22]. In recent years, numerous investigations have demonstrated that calcium carbonate could act as a cost-effective green material to remove heavy

* Corresponding authors.

E-mail address: gtzhou@ustc.edu.cn (G.-T. Zhou).

metals from wastewater [23–31]. For example, waste calcite sludge, an industrial waste material, could be used for the removal of Cd(II), Cu(II), Pb(II), and Zn(II) from aqueous solution [24]. Biogenic aragonite and calcite mollusk shells also exhibited high sorption capacities to Pb(II), Cd(II) and Zn(II) from contaminated water [27]. Hybrid calcite-pepsin hemispheres prepared by vapor-diffused method were applied to the removal of Cu(II) and Pb(II) [28]. Compared with calcite and aragonite, vaterite usually has high specific surface area, high dispersion and small specific gravity [32]. Additionally, the solubility product of vaterite is reported to be $10^{-7.91}$ at 25 °C [33], which is higher than that of calcite ($10^{-8.48}$), aragonite ($10^{-8.34}$), and most heavy metal carbonates like otavite ($10^{-12.10}$), cerussite ($10^{-13.13}$) and smithsonite ($10^{-9.87}$) [23,34,35]. Thermodynamically, hexagonal vaterite is the most unstable phase relative to rhombohedral calcite, otavite, cerussite and smithsonite, as well as orthorhombic aragonite [19]. This fact may facilitate the transformation of vaterite into a heavy metal-rich carbonate in the presence of a solution containing these elements in a similar way to what has been observed for calcite and aragonite [36], enhancing the removal capacity of vaterite to heavy metal ions. Moreover, vaterite-based nanomaterials also exhibit excellent removal performance for dyes [31,37]. Therefore, vaterite may have potential application in the simultaneous removal of heavy metals and dyes from aqueous solution. However, to the best of our knowledge, no research has been reported on the simultaneous removal of heavy metals and dyes by calcium carbonate, especially by vaterite.

In this study, Cd(II) and CR were selected as model pollutants because Cd(II) and CR are typical pollutants in the dye wastewater. For instance, a study from an industrial estate of Mumbai, India suggested that the concentration of Cd(II) is up to 31.0 mg/L in dyes and textile effluents [38]. In addition, Congo red (CR) is reported to be one of the commonest disazo dyes in the wastewaters of textiles, printing, dyeing, paper, rubber and plastics industries [8,9]. Herein, the hierarchical vaterite spherulites, synthesized by a facile injection-precipitation method at room temperature, were applied for simultaneous removal of Cd(II) and CR. The mutual effect between the copollutants in the binary system and the removal mechanism were systematically investigated.

2. Materials and methods

2.1. Materials

All chemical reagents were of analytic reagent grade and used as received without any further purification. CaCl_2 , Na_2CO_3 , CdCl_2 , Congo red (CR), HCl and NaOH were purchased from Sinopharm Chemical Reagent Co., Ltd. Deionized water purchased from Blue Science and Trade Co., Ltd (Anhui, China) was used in all the experiments.

2.2. Preparation of hierarchical vaterite spherulites

Vaterite synthesis experiments were carried out at room temperature by using an injection-precipitation method developed from our previous work [39]. Typically, 0.02 mol of CaCl_2 was dissolved in 220 ml of deionized water in a 250 ml beaker to obtain a homogeneous solution (0.09 mol/L CaCl_2). Then 20 ml of Na_2CO_3 solution (0.5 M) was quickly injected into the CaCl_2 solution under magnetic stirring to form a white precipitate. After being continuously stirred for 2 min, the white precipitate was harvested by filtration, washed with deionized water and absolute ethanol several times, and finally dried in vacuum at room temperature for 12 h.

2.3. Characterization

Several analytical techniques were used to characterize the synthesized products. The powder X-ray diffraction (XRD) patterns of the samples were recorded with a Japan Map AHF X-ray diffractometer equipped with graphite monochromatized Cu $K\alpha$ irradiation ($\lambda = 1.5418 \text{ \AA}$), employing a scanning rate of $0.02^\circ \text{ s}^{-1}$ in the 2θ range of $10\text{--}70^\circ$. FT-IR spectra were measured on a Nicolet Magna IR-750 spectrophotometer from 4000 to 400 cm^{-1} at room temperature. The morphology and microstructure of the products were observed by JEOL JSM-6700F field-emission scanning electron microscopy (FESEM) equipped with X-MAX^N energy dispersed X-ray spectroscopy (EDX, Oxford Instruments). Before the FESEM observation, the samples were loaded on a Cu foil, and then sprayed by Au. X-ray photoelectron spectra (XPS) were taken on a Thermo ESCALAB 250 X-ray photoelectron spectrometer with Al K α radiation. All spectra were calibrated with graphitic carbon as the reference at a binding energy of 284.6 eV to compensate for the surface charging effects. The XPSPEAK 4.1 software was used to fit the XPS spectra of each relevant element into subcomponents. The zeta potential of the materials was determined with NanoBrook Omni Zeta Potential Analyzer (Brookhaven Instruments Corporation, America).

2.4. Removal experiments

The removal behavior of the vaterite spherulites to Cd(II) or CR was firstly investigated individually. All removal experiments were conducted by mixing 0.05 g of the scavenger (vaterite spherulites) with 50 mL of Cd(II) ($C_{\text{Cd(II), initial}} = 500 \text{ mg/L}$) or CR ($C_{\text{CR, initial}} = 20 \text{ mg/L}$) solution at room temperature. To determine the optimal pH condition for the removal, the effect of pH on the removal ability of the scavenger was studied in a pH range of 3.0–7.0 for Cd(II) solution because Cd(OH)_2 can precipitate out of the solution when pH exceeds 8.0 ($K_{\text{sp, Cd(OH)}_2} = 10^{-15.00}$ [40]). A pH range of 3.0–11.0 was adopted for CR solution. The kinetics experiments of Cd(II) or CR sorption by the vaterite spherulites were carried out at 5–150 min. After the established contact time, the precipitate was separated from the mixture by centrifugation at 10,000 rpm for 10 min. The residual concentration of Cd(II) in the supernatant was determined using inductively coupled plasma atomic emission spectroscopy (ICP-AES, Optima 7300 DV). Inductively coupled plasma mass spectrometry (ICP-MS, Plasma Quad3) was used when the concentration of Cd(II) was below 0.1 mg/L. The Ca(II) concentration released from the vaterite was also measured by the same techniques as the Cd(II). Residual dye CR concentration in the supernatant was determined by UV–vis spectrometry (TU-1901, Beijing Purkinje General Instrument Co., Ltd.) at a wavelength of the maximum absorbance of CR ($\lambda_{\text{max}} = 497 \text{ nm}$). In addition, to understand the mutual effect of the concurrent Cd(II) and CR on their removal by vaterite, a series of binary sorption experiments were performed by varying Cd(II) (0–1800 mg/L) or CR (0–300 mg/L) concentration with another one fixed at pH 6.0. All removal experiments were run in triplicate, and averaged values were reported. The removal capacity q_e (mg/g) and removal percentage $W\%$ was calculated according to following equations, respectively:

$$q_e = \frac{(C_i - C_e)V}{m} \quad (1)$$

$$W\% = \frac{(C_i - C_t)100\%}{C_i} \quad (2)$$

where C_i (mg/L), C_e (mg/L) and C_t (mg/L) are the liquid phase concentration of Cd(II) or CR at initial, equilibrium and any time t , respectively. V is the volume of the solution (L), and m is the mass of vaterite spherulites added (g).

The saturation indexes with respect to vaterite (SI_{vat}) and otavite (SI_{ota}) at different time intervals were calculated by using the program Visual MINTEQ version 3.1. The thermodynamic database for the components, aqueous species and the mineral phase solubility were from the default comp_2008.vdb, thermo.vdb and type6.vdb files, respectively. The concentrations of the aqueous species and pH were input into the model. Besides, the temperature was kept constant at 25 °C, and the oversaturated solids were allowed to precipitate.

3. Results and discussion

3.1. Characterization of the synthesized vaterite spherulites

Fig. 1a and b depict the typical FESEM images of the synthesized products. The panoramic FESEM image in Fig. 1a shows that the

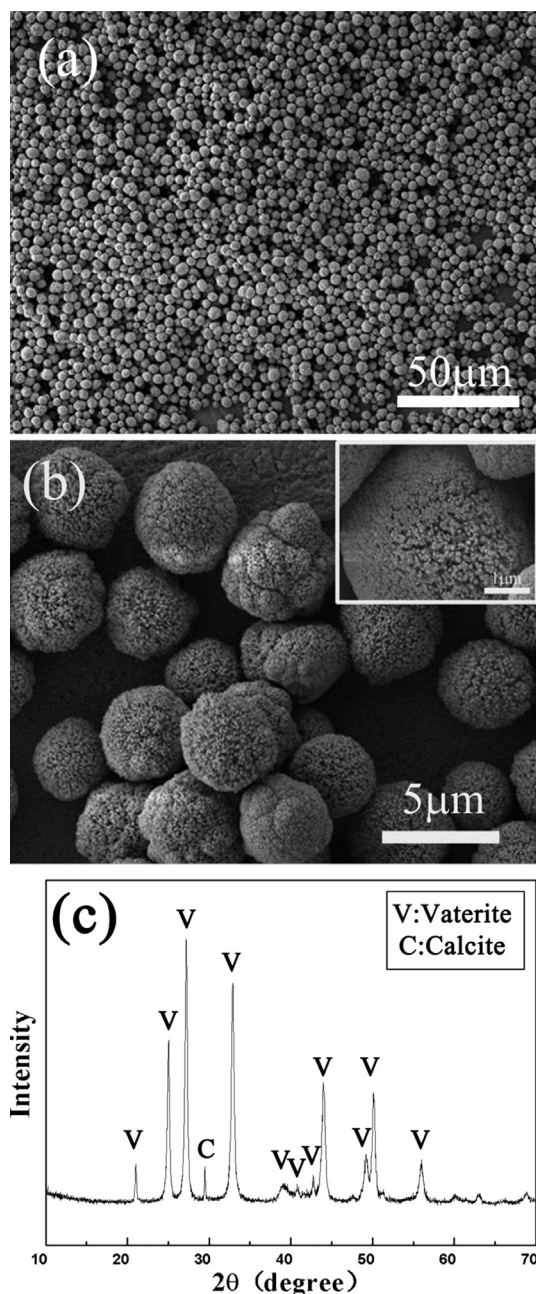


Fig. 1. Typical FESEM images (a, b) and XRD pattern (c) of the obtained vaterite spherulites.

white precipitate is composed of a large quantity of well-dispersed microspheres with diameters of 3.0–4.0 μm. Further enlarged FESEM image reveals that the microspheres are a hierarchical architecture that results from the aggregation of nanocrystals about 20 nm in size, exhibiting a spherulite-like structure (Fig. 1b and its inset). Furthermore, composition and phase purity of the product were examined by XRD and FT-IR techniques. The representative XRD pattern (Fig. 1c) unveils that the product is mainly hexagonal vaterite with the lattice parameters $a = 7.147$ Å, $c = 16.917$ Å, and space group $P6_3/mmc$ (JCPDS file 33-0268), except for a trait of calcite (JCPDS file 83-0578), confirming that the spherulites are vaterite-type CaCO_3 . The sharp and strong peaks also show that the product is well-crystallized. In addition, the corresponding FT-IR spectrum is exhibited in Fig. 2a. The strong vibrational bands at 1084, 875, and 746 cm^{-1} can unambiguously be assigned to carbonate symmetric stretching (ν_1 mode), carbonate out-of-plane bending (ν_2 mode), and in-plane bending (ν_4 mode) vibrations of vaterite, respectively [39,41], further confirming that the spherulite-like structure is vaterite. A very weak peak belonging to calcite at 711 cm^{-1} is also detected (Fig. 2a) [42], corroborating that calcite is of trace, which is consistent with the XRD result (Fig. 1c). Therefore, the SEM, XRD, and FT-IR results demonstrate that the preparation of the hierarchical vaterite spherulites can be easily achieved by the method performed here.

3.2. Sole Cd(II) removal

It's well known that vaterite would gradually dissolve at low pH conditions, and precipitation of hydroxide of heavy metal ions would occur at high pH values. Therefore, the parameter pH is usually believed to be one of the most important factors affecting the removal process [43]. Herein, the effect of pH on the removal of Cd(II) by vaterite was investigated at an initial pH ranging from 3.0 to 7.0, an initial Cd(II) concentration of 500 mg/L and a contact time of 12 h. As shown in Fig. 3a (bluish notation), the removal percentage of Cd(II) is found to significantly increase with the initial pH

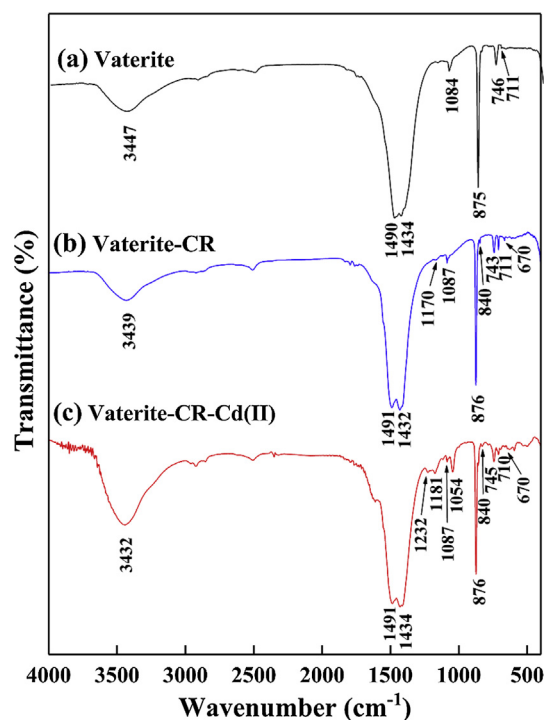


Fig. 2. FT-IR spectrum of the vaterite spherulites (a), the vaterite scavenger after 12 h treatment of 50 mg/L CR (b), and the vaterite scavenger after 12 h treatment of 50 mg/L CR and 1500 mg/L Cd(II) (c).

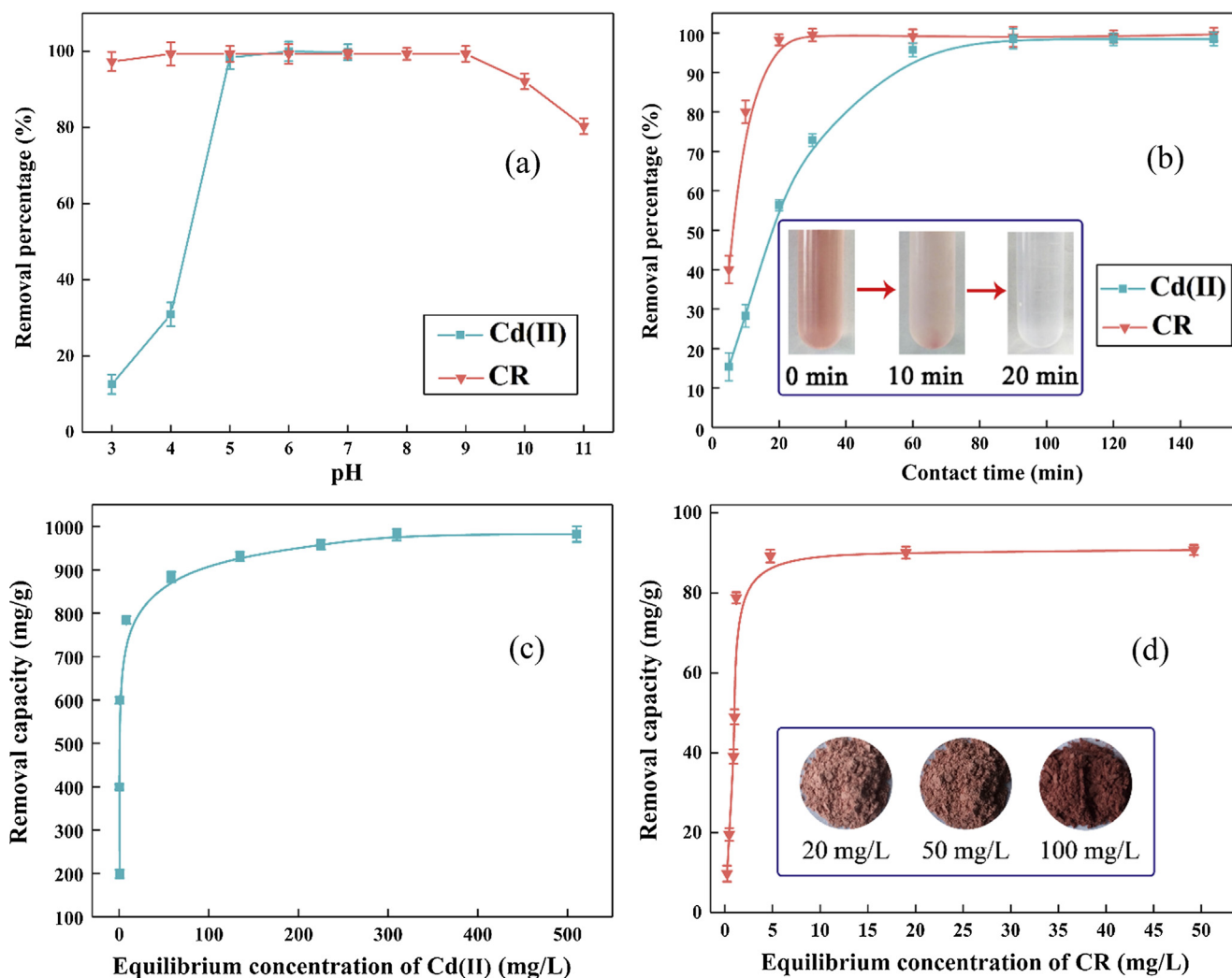


Fig. 3. Effects of initial pH (a) and contact time (b) on the removal of Cd(II)/CR by the vaterite spherulites; sorption isotherms of Cd(II) (c) and CR (d). Inset in Fig. 3b: the digital images of solution collected at different contact time. Inset in Fig. 3d: the color of the scavenger collected from the solution with different CR concentration.

and to approach 100% at pH 5.0. Thereafter, it doesn't change very much with further increasing the pH to 7.0. Consequently, it can be concluded that the removal of Cd(II) by the vaterite spherulites is highly dependent on initial pH of the solution, and initial pH 6.0 was selected in the subsequent Cd(II) removal experiments.

The removal kinetics of Cd(II) by the vaterite spherulites was studied at an initial Cd(II) concentration 500 mg/L, initial pH 6.0 and contact time 0–150 min. One can find from Fig. 3b (blue notation) that a fast Cd(II) removal phase occurs in the first 60 min, and reaches a plateau after subsequent 30 min, indicating a high removal efficiency of vaterite to Cd(II). The initial fast removal rate of Cd(II) could be ascribed to the higher solubility of vaterite relative to otavite (CdCO_3) and the hierarchical structure of the vaterite spherulites. During the Cd^{2+} removal process, the initial dissolution of the vaterite provides enough CO_3^{2-} ions for the precipitation of CdCO_3 phase. This facilitates Cd(II) precipitation on the surfaces of the vaterite spherulites. With the surface of vaterite covered by the precipitated CdCO_3 , the dissolution rate of the vaterite spherulites would gradually decrease, and thus the removal rate of Cd(II) slows down. Fig. S1 also depicts the concentration evolution of Cd(II) and Ca(II) in solution at different treatment times. It unambiguously exhibits a reverse evolution trend, and the content of dissolved Ca(II) is 4.45 mM after 3 h of treatment, very close to the removed Cd(II) (4.31 mM), demonstrating

that the removal of Cd^{2+} in solution predominantly proceeds via a transformation from vaterite to otavite. Furthermore, the saturation indexes with respect to the vaterite (SI_{vat}) and otavite (SI_{ota}) at different time intervals (Fig. S2), calculated by program Visual MINTEQ version 3.1, show that at the very beginning of the removal treatment, the solution is obviously undersaturated either for vaterite or otavite, but the fast dissolution of the vaterite spherulite ($SI_{\text{vat}} < 0$) leads to a dramatic increase in SI_{ota} , and the solution becomes quickly supersaturated for otavite, reaching a maximum SI_{ota} 2.89 at 30 min. It further supports the Cd^{2+} removal by otavite precipitation. Afterwards, the continuous precipitation and growth of otavite lead to the decrease of Cd(II) concentration in solution, and the SI_{ota} gradually approaches zero, showing an equilibrium state.

In addition, sorption isotherm of vaterite spherulites to Cd(II), studied at contact time 12 h, initial pH 6.0 and initial Cd(II) concentration ranging from 100 to 1500 mg/L, reveals that the maximum removal capacity is ca. 984.5 mg/g (Fig. 3c), which is higher than or comparable to those of previous reported materials, such as EDTA functionalized magnetic iron oxide nanoparticles (79.4 mg/g) [44], carboxyl modified lingocellulose-biomass jute fiber (89.0 mg/g) [45], polyaniline grafted chitosan (14.3 mg/g) [46], and other CaCO_3 -based materials like natural calcite (18.5 mg/g) [25], nano-sized aragonite mollusk shell (997.9 mg/g) [29], amorphous

Table 1
Comparison of the maximum removal capacity of Cd(II) by various scavengers.

Scavengers	Maximum removal capacity of Cd ²⁺ (mg/g)	Ref.
EDTA functionalized magnetic nanoparticle	79.4	[44]
Carboxyl modified lignocellulose-biomass jute fiber	89.0	[45]
Polyaniline grafted chitosan	14.3	[46]
Natural calcite	18.5	[25]
Nano-sized aragonite mollusk shell	997.9	[29]
Amorphous calcium carbonate	514.6	[26]
Hierarchical vaterite-maltose	487.8	[47]
Hierarchical porous vaterite	1040	[31]
Vaterite spherulite	984.5	This work

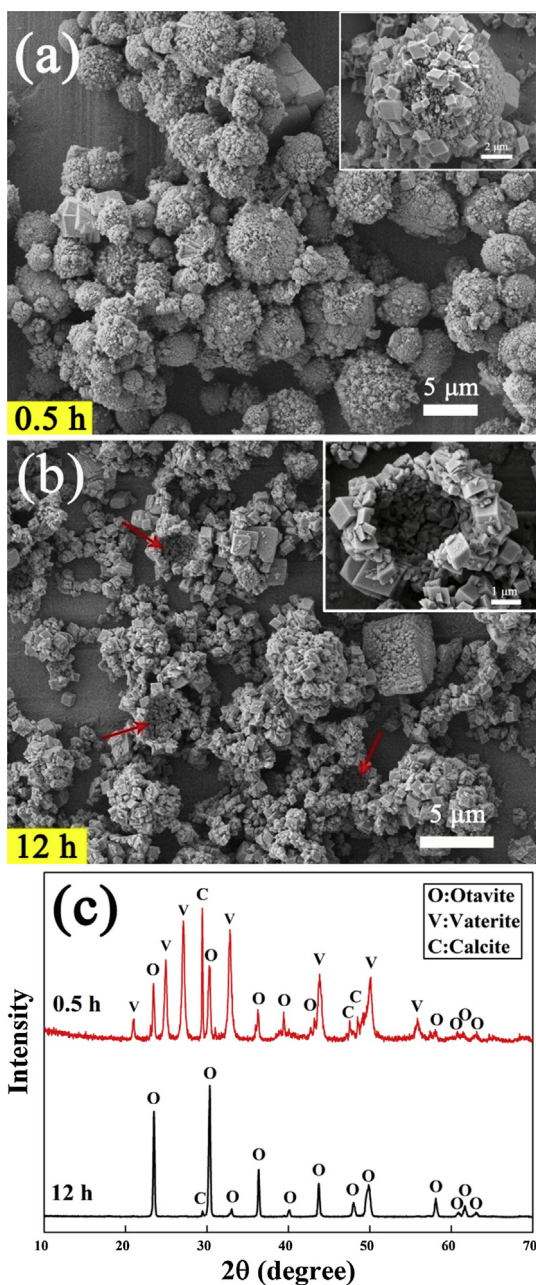


Fig. 4. FESEM images (a, b) and XRD patterns (c) of the scavenger collected after 0.5 h and 12 h treatment of Cd(II) in sole Cd(II) system ($C_{Cd(II), initial} = 1000$ mg/L).

calcium carbonate stabilized by polyacrylic acid (514.6 mg/g) [26], vaterite-maltose hybrid materials synthesized by a 24 h gas-diffusion method (487.8 mg/g) [47], and vaterite microsphere synthesized in dimethylformamide-water (DMF-H₂O) mixed solvent at 130 °C for 4 h (1040 mg/g) [31], as summarized in Table 1. Therefore, the hierarchical vaterite spherulites could be used as an effective scavenger for Cd(II) removal from aqueous solution.

At present, a general consensus is that the removal of divalent metal ions by calcium carbonate usually proceeds through a precipitate-transformation process [27,29,36,48]. In our study,

Table 2
Comparison of the maximum removal capacity of CR by various scavengers.

Scavengers	Maximum removal capacity of CR (mg/g)	Ref.
Jujuba seeds	56.0	[50]
Fe ₃ O ₄ @graphene	33.6	[51]
Hollow Zn-Fe ₂ O ₄ nanospheres	16.6	[9]
Fe ₃ O ₄ @SiO ₂	54.6	[52]
pTSA-Pani@GO-CNT	66.7	[53]
CoFe ₂ O ₄ /rGO	104.5	[54]
Vaterite spherulite	89.0	This work

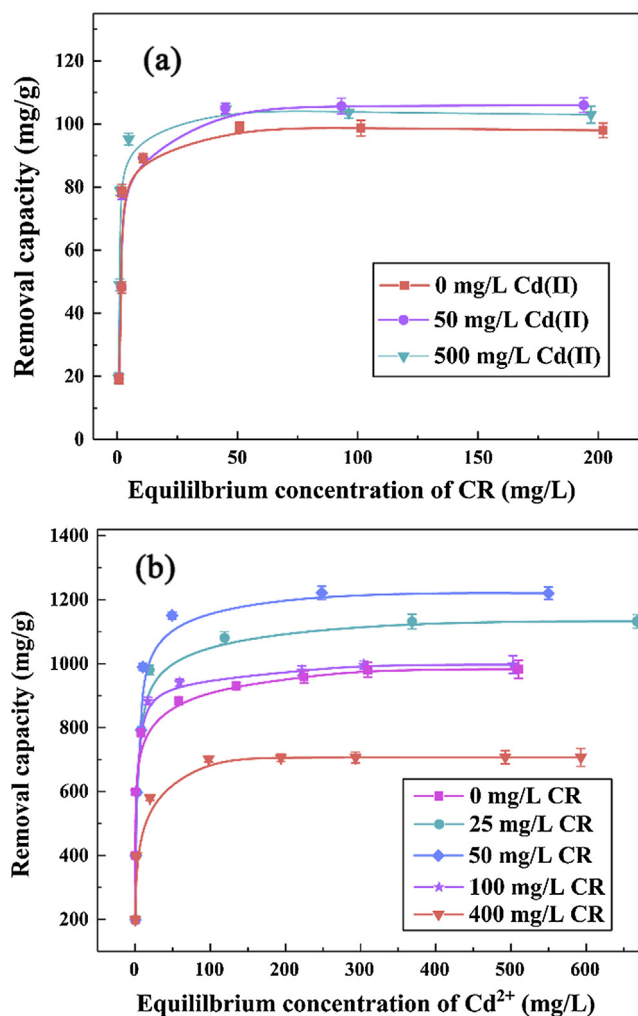


Fig. 5. Sorption isotherms of CR (a) and Cd(II) (b) by the vaterite spherulites in the binary Cd(II)-CR system at pH 6.0; (a) $C_{Cd(II), initial}$: 0, 50, 500 mg/L, $C_{CR, initial}$: 0–300 mg/L; (b) $C_{CR, initial}$: 0, 25, 50, 100, 400 mg/L, $C_{Cd(II), initial}$: 0–1800 mg/L.

because of the initial dissolution of vaterite spherulites, the concentration of CO_3^{2-} ions on the surfaces and around vaterite spherulites may be relatively higher than those in bulk solution. As a consequence, Cd(II) ions in aqueous solution can combine with the dissociated CO_3^{2-} to form insoluble otavite (CdCO_3) depositing on the surfaces of vaterite spherulites. For otavite (CdCO_3), it is isostructural with calcite (space group $R\text{-}3c$), and the lattice mismatch between otavite and calcite is small [27,29,36]. Therefore, the low uptake capacity and slow removal kinetics of Cd(II) by calcite occurs because of a two dimensional epitaxial growth of otavite on the calcite surface [36]. This can significantly passivate the underlying surface and slow the dissolution rate of the underlying mineral calcite [36,48]. In contrast, vaterite possess hexagonal structure with a space group $P6_3/mmc$, and thus otavite will precipitate by a random three dimensional heterogeneous nucleation rather than the lattice match epitaxial growth onto the surface of vaterite, leaving some pore spaces at the otavite-vaterite interface. This allows for the vaterite to continue dissolution and to be less affected by the precipitated otavite. Similar random three dimensional heterogeneous nucleation and growth has been also observed in the sorption experiment of Cd(II) by biogenic aragonite [36]. Such three dimensional heterogeneous nucleation and growth can be observed by FESEM. As shown in Fig. 4a, numerous rhombohedra with side length of ca. 500 nm form on the surface of spherulite-like structures after 0.5 h of contact with 1000 mg/L of Cd(II) solution. The XRD analyses identify the appearance of a neo-mineral otavite (JCPDS file 42-1342) (Fig. 4c), indicating that the small rhombohedra stuck to the spherulites are otavite. When the treatment time prolongs to 12 h, the vaterite spherulites disappear completely, and hollow spherical structures consisting of small otavite rhombohedra form (Fig. 4b and c). In particular, the diameters of hollow spherical structures are about 3 μm (inset in

Fig. 4b), which match the size of the initial vaterite spherulites (Fig. 1b). This confirms that the Cd(II) removal process occurs on/near the vaterite surfaces through a continuous dissolution of vaterite and precipitation of otavite by a random three dimensional heterogeneous nucleation and growth on the surface of vaterite, leading to an efficient Cd(II) removal. On the other hand, the difference of the solubility product between vaterite ($10^{-7.91}$) and otavite ($10^{-12.10}$) is larger than that of calcite ($10^{-8.48}$) and otavite [23,34], and thus the transformation from vaterite to otavite is much easier than calcite. In a word, the hierarchical structure of vaterite, crystallographic mismatch of vaterite with calcite, and the larger Ksp of vaterite relative to otavite result in a high removal rate and capacity of the vaterite spherulites to Cd(II).

3.3. Sole CR removal

As for sole CR system, a series of pH-dependent removal experiments were firstly conducted at initial pH from 3.0 to 11.0, CR concentration 20 mg/L, and contact time 12 h. As shown in Fig. 3a (pinkish notation), CR can be almost completely removed over the pH range from 3.0 to 9.0, but then declines with pH further increasing from 9.0 to 11.0, indicating that high initial pH is unfavorable to the sorption. It's well known that the sorption is dependent on the surface charge of sorbent, and surface charge of a material is neutral at the point of zero charge (PZC), but positive below the pHpzc. Here, the pHpzc of the vaterite spherulites was measured to be about 9.88 (Fig. S3), which is consistent with the previous study (pHpzc = 9.90) [49]. Such a high pHpzc facilitates the high uptake of anionic dye CR due to the strong electrostatic attraction between anionic CR and vaterite with positive charge. However, as the pH further increases, the positive charge of the vaterite surface decreases (Fig. S3). As a result, the

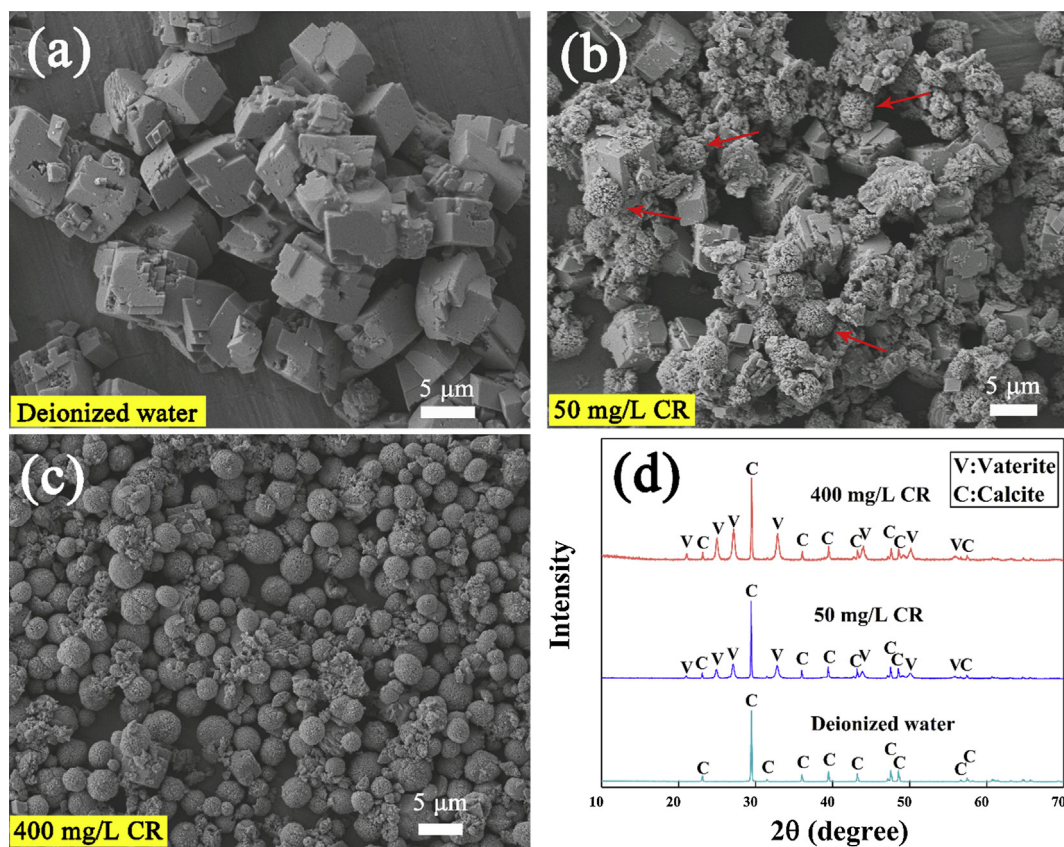


Fig. 6. FESEM images (a, b, c) and XRD patterns (d) of the scavenger spherulites after 12 h treatment of deionized water (a), 50 mg/L CR solution (b) and 400 mg/L CR solution (c).

electrostatic attraction between CR and vaterite will be weakened, leading to the lower uptake of CR. Considering the excellent CR removal performance over the initial pH range from 3.0 to 9.0, pH 6.0 was selected in the following CR removal experiments.

Fig. 3b (pinkish notation) depicts the time profile of CR sorption by the vaterite spherulites at CR concentration 20 mg/L, initial pH 6.0 and contact time 0–150 min. The removal percentage of CR has reached 80% within the first 10 min, and CR can be completely removed after subsequent 10 min, exhibiting an extremely high removal efficiency. The rapid sorption process can be also visually seen by the digital images of the supernatants collected at different contact times (inset in Fig. 3b), showing that a 20 min of treatment has led to clarification of the solution. In addition, after sorption treatment, the precipitate color has turned into pinkish, entirely different from the white vaterite, and the color gradually becomes darker with the incremental CR concentration (inset in Fig. 3d). These indicate the efficient immobilization of CR by the vaterite. The sorption isotherm also shows that the maximum removal capacity of CR by the vaterite spherulites is ca. 89.0 mg/g (Fig. 3d), which is higher than or comparable to that of previous reported adsorbents, such as jujuba seeds (56.0 mg/g) [50], Fe₃O₄@graphene (33.6 mg/g) [51], hollow Zn-Fe₂O₄ nanospheres (16.6 mg/g) [9], Fe₃O₄@SiO₂ (54.6 mg/g) [52], pTSA-Pani@GO-CNT (66.7 mg/g) [53] and CoFe₂O₄/rGO (104.5 mg/g) [54], as listed in Table 2. Therefore, the as-synthesized vaterite spherulites can be potentially applied to the CR removal from aqueous solution.

3.4. Simultaneous removal of Cd(II) and CR

In practical wastewater, heavy metal Cd(II) has been reported to be often concomitant with organic dyes in dye wastewater [16]. Thus, exploring facile and environmentally benign materials for synergic removal of Cd(II) and CR is of considerable practical interest during wastewater treatment.

Sorption isotherms of Cd(II) and CR by the vaterite spherulites in the binary system were investigated by varying CR or Cd(II) concentration with another one fixed. In addition, according to the pH-dependent experiments of sole Cd(II) and CR removal, the excellent Cd(II) or CR removal by the vaterite can be achieved in the pH range of 5–7 (Fig. 3a). Therefore, pH 6.0 is selected in the current binary removal experiments. One can find from Fig. 5a that the concurrent Cd(II) shows negligible effect on CR removal. This is because that at pH 6.0 the surfaces of vaterite spherulites have positive charge, showing a preferential sorption to anionic CR. In addition, the subsequent depositing of CdCO₃ on the vaterite spherulites will also provide extra active sites for the sorption of CR due to similar pH_{zpc} of otavite (9.52) to vaterite (9.88) (Fig. S3). As a result, concurrent Cd(II) almost has no effect on CR removal even the vaterite surfaces are continuously covered by the precipitating CdCO₃. On the contrary, however, the removal of Cd(II) is highly affected by the concurrent CR, exhibiting significant enhancement at lower CR concentration (<100 mg/L) and inhibition at higher CR concentration (>100 mg/L) (Fig. 5b). Specifically, the removal capacity of Cd(II) increases from 982.7 mg/g without CR to 1220.2 mg/g with 50 mg/L CR, but reduces to 703.5 mg/g with 400 mg/L CR, which is 71.6% of that without CR (Fig. 5b). This remarkable influence of CR on the Cd(II) removal may be attributed to the preferential adsorption and subsequent stabilization of CR to vaterite. As we know, thermodynamically unstable vaterite can easily transform into stable calcite in solution through a dissolution/recrystallization process [39,55]. Our experiment results also show that the vaterite spherulites dispersed in deionized water have completely transformed into rhombohedral calcite after 12 h of stirring (Fig. 6a and d). Nevertheless, in the presence of 50 mg/L CR, the same stirring time donates a coexistence of rhombohedral calcite and spherulite-like vaterite

(Fig. 6b and d), indicating that dye CR molecules can stabilize the vaterite in solution. Further increasing CR concentration to 400 mg/L, FESEM and XRD analyses (Fig. 6c and d) reveal that except for a small quantity of calcite, vaterite spherulites predominate yet in the sample. Moreover, the FT-IR spectrum also shows that besides the strong characteristic vibrations belonging to vaterite, the weak vibrational bands of the sulfonic acid group at 1170 cm⁻¹ and the benzene framework at 840 and 670 cm⁻¹ are detected out in the sample (Fig. 2b) [56,57], indicating that the CR molecules are intimately associated with vaterite. These results

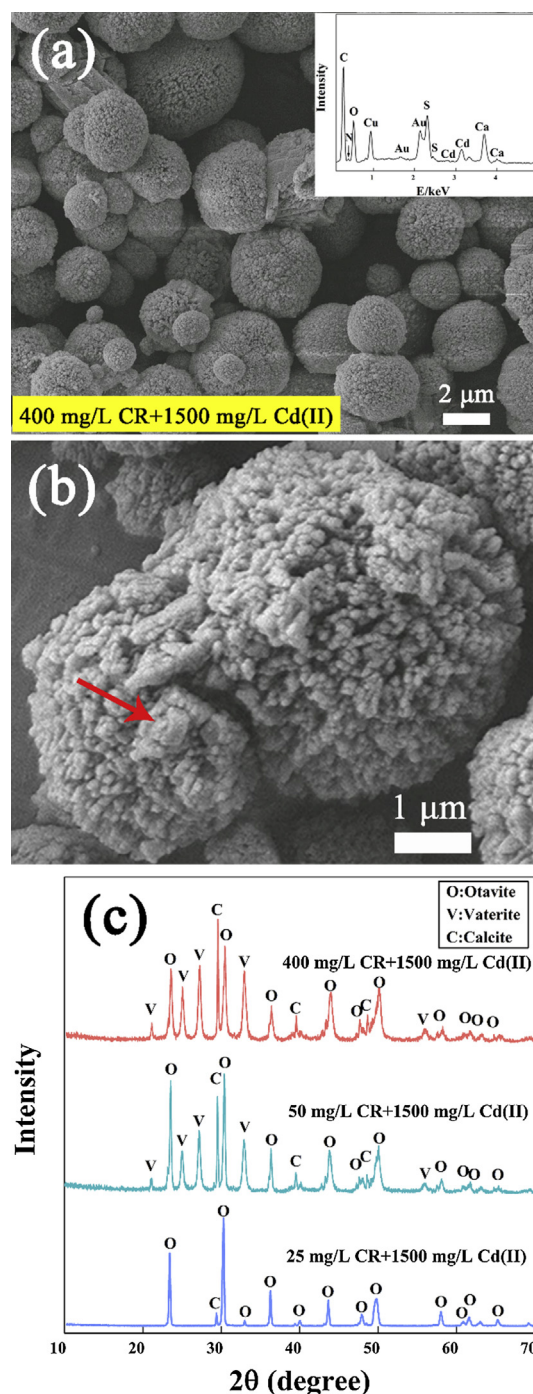


Fig. 7. FESEM image of the scavenger after 12 h treatment in the binary system with 400 mg/L CR and 1500 mg/L Cd(II) (a). XRD patterns of the scavenger after 12 h treatment of 25 mg/L, 50 mg/L and 400 mg/L CR with fixed Cd(II) concentration of 1500 mg/L (b).

demonstrate that the CR molecules adsorbed onto the surfaces of vaterite spherulites could obstruct the transformation from vaterite to calcite. It has been documented that many organic additives with sulfonic group can stabilize metastable vaterite in solution [58–60]. For instance, by introducing poly (vinylsulfonic acid) (PVA) during the synthesis process, Nagaraja et al. obtained vaterite nanoparticles that could be maintained in solution for at least 5 months [58]. In the presence of sodium lignosulfonate (SLS), the vaterite with multilayered structures could be kept for two months

in the mother solution [59]. Here, CR molecules may exert the similar stabilization to the vaterite spherulites by their inherent sulfonic groups (Fig. S4), leading to the low dissolution of vaterite. This stabilization phenomenon occurs in the binary Cd(II)-CR system as well. After 12 h treatment of 400 mg/L CR and 1500 mg/L Cd(II), the vaterite spherulites predominate in sight with fewer small otavite rhombohedra (Fig. 7a-c). Corresponding EDX spectrum also presents the significant Ca, N and S, as well as weak Cd signals (inset in Fig. 7a), confirming the efficient adsorption of CR

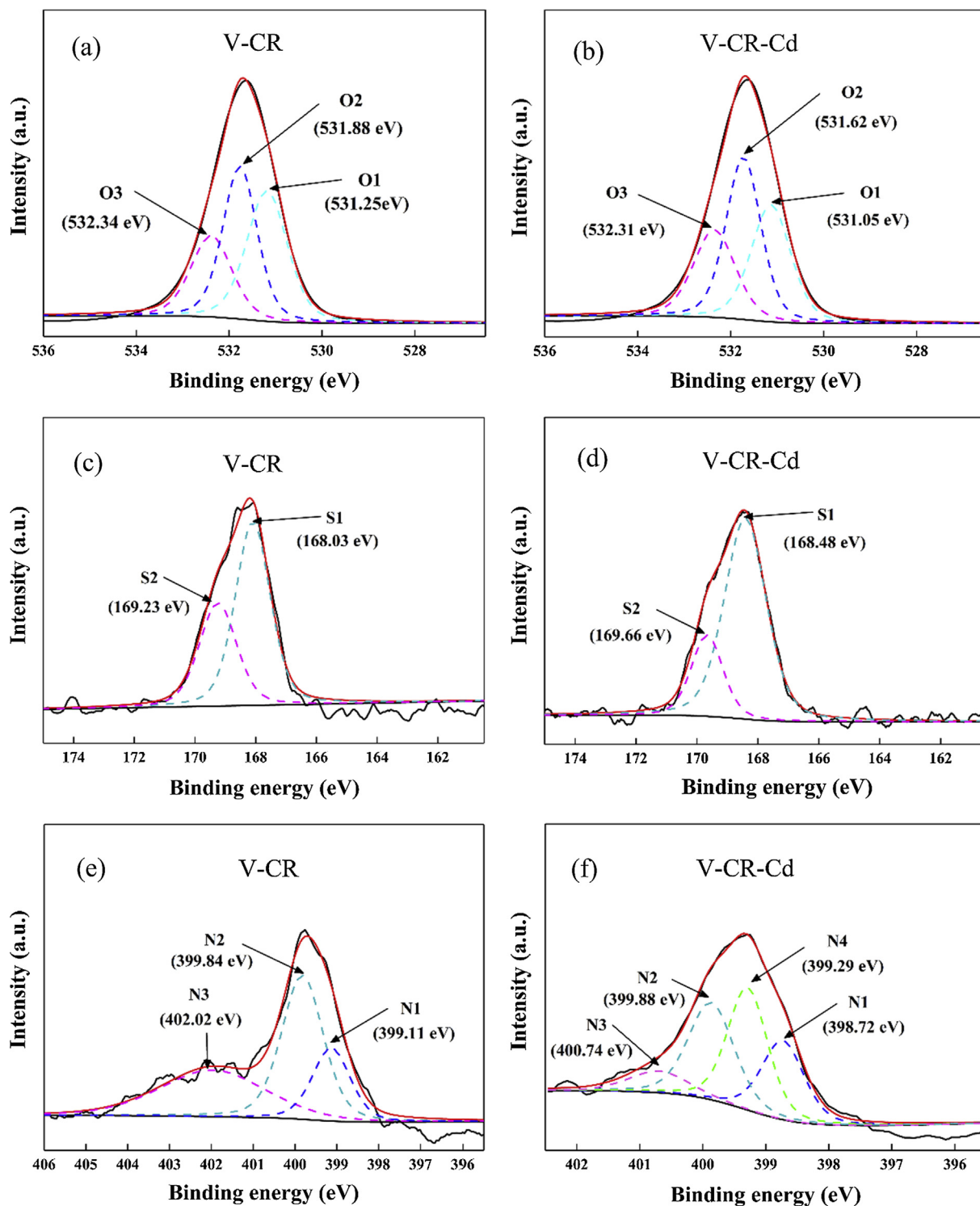


Fig. 8. XPS spectra of O1s (a, b), S2p (c, d) and N1s (e, f) in the sample V-CR ($C_{CR,initial} = 50$ mg/L) and sample V-CR-Cd ($C_{CR,initial} = 50$ mg/L, $C_{Cd(II), initial} = 1500$ mg/L). Energy range: 0–1350 eV.

and suppressed removal of Cd(II) by vaterite at higher CR concentration (Fig. 5b). It appears that at higher CR concentration (>100 mg/L), CR exerts strong stabilization to the vaterite spherulites, and thus the Cd(II) removal through the transformation of vaterite into otavite is hindered. As a result, the deteriorated removal performance for Cd(II) occurs.

In contrast, at lower CR concentration (e.g., 25 and 50 mg/L), a significantly incremental Cd(II) removal can be harvested (Fig. 5b). Such phenomenon can be explained as follows: On the one hand, CR at lower concentration cannot enough stabilize the vaterite spherulites, which can be supported by the FESEM and XRD results (e.g., Figs. 7c and S5). For instance, at 25 mg/L CR, all the vaterite spherulites have transformed into otavite rhombohedra after 12 h sorption treatment (Figs. 7c and S5a), but vaterite and otavite coexist at 50 mg/L CR (Figs. 7c and S5b). In this case, considerable Cd(II) can be immobilized by the transformation from vaterite into otavite. On the other hand, the CR molecules adsorbed on the vaterite or neo-otavite have strong coordination with Cd(II) by their amino and sulfonic groups, thereby offering additional functional groups for capturing Cd(II). This is further supported by the FT-IR analysis of the used scavengers. Compared with the FT-IR spectrum of the sample obtained in the sole CR solution, a evidently bathochromic shift of the stretching vibration of the sulfonic acid group from 1170 to 1181 cm^{-1} occurs (Fig. 2b and c), indicating that the interactions between Cd(II) and sulfonic acid groups of the adsorbed CR may occur. To further identify the possible functional groups of CR molecules involved in the promotional Cd(II) removal, the XPS analyses of the used scavengers obtained in the sole CR (sample V-CR) and binary Cd(II)-CR (sample V-CR-Cd) systems were also conducted, respectively. For sample V-CR, the XPS spectrum of O1s can be deconvoluted into three different peaks (Fig. 8a). Peaks of O1 (531.25 eV) and O3 (532.34 eV) are related to carbonate (CO_3^{2-}) of vaterite [61]. Peak of O2 (531.88 eV) can be assigned to sulfonic group ($-\text{SO}_3^-$) of CR molecules [16]. After removal treatment of concurrent Cd(II) and CR by the vaterite (i.e., sample V-CR-Cd), however, the peak of O1 shifts to lower binding energy of 531.05 eV (Fig. 8b). This is close to that of CO_3^{2-} in the otavite [62], which can be attributed to the partial transformation of vaterite to otavite (Fig. 7c and S5b). Meanwhile, the peak of O2 shifts to 531.62 eV (Fig. 8b), indicating a direct coordination of oxygen in sulfonic group of CR with Cd(II). Furthermore, S2p spectra of samples V-CR and V-CR-Cd (Fig. 8c and d) can be also deconvoluted into two peaks S1 and S2, corresponding to two sulfuric groups in CR molecules (Fig. S4) [63]. In the presence of Cd^{2+} , however, the peaks of S1 and S2 shift from 168.03 and 169.23 to 168.48 and 169.66 eV, respectively (Fig. 8c and d), further suggesting that sulfuric groups in the CR molecules adsorbed on the spherulites involve in Cd immobilization. Similarly, the deconvolution of N1s peak either for sample V-CR or V-CR-Cd was also performed. As shown in Fig. 8e and f, the fitted N1s peak in sample V-CR can be assigned to amino ($-\text{NH}_2$, N1), azo ($-\text{N}=\text{N}-$, N2) and protonated amine ($-\text{NH}_3^+$ or $-\text{NH}_2^+$, N3) of CR molecules [16,64,65]. Compared with sample V-CR, nevertheless, a new peak at 399.29 eV appears in sample V-CR-Cd, and the position of N2 changes little, but the N1 and N3 evidently shift from 399.11 and 402.02 to 398.72 and 400.74 eV (Fig. 8f). These differences indicate that the coordination between Cd(II) and amino group ($-\text{NH}_2$) should occur, where N atom donates a lone pair electrons to form the covalent bond N—Cd, causing the reduction of electron cloud density [66,67]. The similar coordinations have been also observed between Cu^{2+} and acid black 1 with sulfuric and amino groups by XPS technique [16]. Therefore, sulfuric and amino groups in the adsorbed CR molecules are responsible for the enhanced Cd(II) removal in the binary system. On the basis of our results, it can be safely concluded that the simultaneous removal of Cd(II) and CR by the vaterite spherulites is through a multistep process,

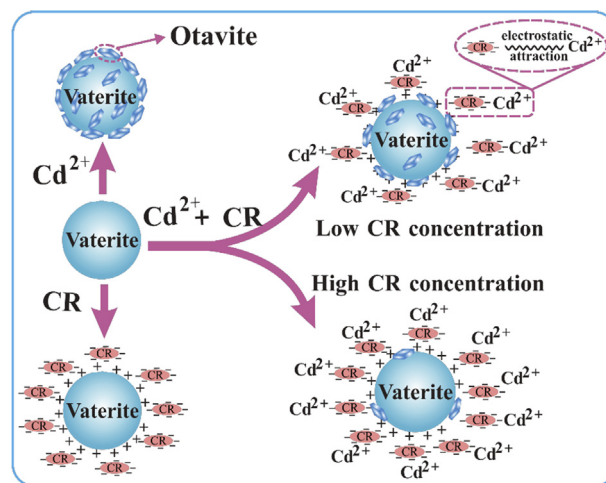


Fig. 9. Schematic mechanism for the simultaneous removal of Cd(II) and CR by the vaterite spherulites in the binary Cd(II)-CR solution.

including preferential adsorption of dye CR, stabilization of CR to vaterite, coordination of the adsorbed CR molecules with Cd(II), and transformation of vaterite into otavite, as illustrated in Fig. 9.

4. Conclusion

In summary, the vaterite spherulites, prepared via injection-precipitation method, can potentially used to the simultaneous removal of Cd(II) and CR from aqueous solution. In the sole system, the as-prepared product shows excellent removal performance for Cd(II) and CR, respectively. In the binary Cd(II)-CR system, the removal of Cd(II) is significantly enhanced at lower CR concentration (<100 mg/L), but inhibited with further increase in the CR concentration (>100 mg/L). In addition, the concurrent Cd(II) shows negligible effect on CR removal. The simultaneous removal mechanism involves a series of processes including preferential adsorption of dye CR, stabilization of CR to vaterite, coordination of the adsorbed CR molecules with Cd(II), and transformation of vaterite into otavite. In a word, this study may provide new insights into the simultaneous removal of heavy metal ions and dyes by carbonates, and our results could be further employed in the practical application for integrative and efficient treatment of complicated wastewater.

Acknowledgements

This work was partially supported by the Natural Science Foundation of China (41372053, 41572026), the Chinese Ministry of Science and Technology (2014CB846003), and the Fundamental Research Funds for the Central Universities.

Appendix A. Supplementary material

Supplementary data associated with this article can be found, in the online version, at <https://doi.org/10.1016/j.apsusc.2018.03.081>.

References

- [1] B.K. Körbahti, K. Artut, C. Geçgel, A. Özer, Electrochemical decolorization of textile dyes and removal of metal ions from textile dye and metal ion binary mixtures, *Chem. Eng. J.* 173 (2011) 677–688.
- [2] J. Li, Q.H. Fan, Y.J. Wu, X.X. Wang, C.L. Chen, Z.Y. Tang, X.K. Wang, Magnetic polydopamine decorated with Mg-Al LDH nanoflakes as a novel bio-based adsorbent for simultaneous removal of potentially toxic metals and anionic dyes, *J. Mater. Chem. A* 4 (2016) 1737–1746.

- [3] F.P. Zhao, E. Repo, D.L. Yin, Y. Meng, S. Jafari, M. Sillanpaa, EDTA-cross-linked beta-cyclodextrin: an environmentally friendly bifunctional adsorbent for simultaneous adsorption of metals and cationic dyes, *Environ. Sci. Technol.* 49 (2015) 10570–10580.
- [4] K. Malachova, Z. Rybkova, H. Sezimova, J. Cerven, C. Novotny, Biodegradation and detoxification potential of rotating biological contactor (RBC) with *Irpex lacteus* for remediation of dye-containing wastewater, *Water. Res.* 47 (2013) 7143–7148.
- [5] C.S. Lei, M. Pi, P.Y. Kuang, Y.Q. Guo, F.G. Zhang, Organic dye removal from aqueous solutions by hierarchical calcined Ni-Fe layered double hydroxide: isotherm, kinetic and mechanism studies, *J. Colloid Interface Sci.* 496 (2017) 158–166.
- [6] R.R. Shan, L.G. Yan, K. Yang, Y.F. Hao, B. Du, Adsorption of Cd(II) by Mg-Al-CO₃- and magnetic Fe₃O₄/Mg-Al-CO₃-layered double hydroxides: kinetic, isothermal, thermodynamic and mechanistic studies, *J. Hazard. Mater.* 299 (2015) 42–49.
- [7] M.M.S. Saif, N.S. Kumar, M.N.V. Prasad, Binding of cadmium to Strychnos potatorum seed proteins in aqueous solution: adsorption kinetics and relevance to water purification, *Colloids Surf., B* 94 (2012) 73–79.
- [8] M.K. Purkait, A. Maiti, S. DasGupta, S. De, Removal of congo red using activated carbon and its regeneration, *J. Hazard. Mater.* 145 (2007) 287–295.
- [9] R. Rahimi, H. Kerdari, M. Rabbani, M. Shafiee, Synthesis, characterization and adsorbing properties of hollow Zn-Fe₂O₄ nanospheres on removal of Congo red from aqueous solution, *Desalination* 280 (2011) 412–418.
- [10] C. Zhang, Z.G. Yu, G.M. Zeng, B.B. Huang, H.R. Dong, J.H. Huang, Z.Z. Yang, J.J. Wei, L. Hu, Q. Zhang, Phase transformation of crystalline iron oxides and their adsorption abilities for Pb and Cd, *Chem. Eng. J.* 284 (2016) 247–259.
- [11] M. Machida, B. Fotoohi, Y. Amamo, L. Mercier, Cadmium(II) and lead(II) adsorption onto hetero-atom functional mesoporous silica and activated carbon, *Appl. Surf. Sci.* 258 (2012) 7389–7394.
- [12] I.M. Ahmed, M.S. Gasser, Adsorption study of anionic reactive dye from aqueous solution to Mg-Fe-CO₃ layered double hydroxide (LDH), *Appl. Surf. Sci.* 259 (2012) 650–656.
- [13] M.D. Liu, J. Xu, B. Cheng, W.K. Ho, J.G. Yu, Synthesis and adsorption performance of Mg(OH)₂ hexagonal nanosheet-graphene oxide composites, *Appl. Surf. Sci.* 332 (2015) 121–129.
- [14] M.E. Skold, G.D. Thyne, J.W. Drexler, D.L. Macalady, J.E. McCray, Enhanced solubilization of a metal-organic contaminant mixture (Pb, Sr, Zn, and perchloroethylene) by cyclodextrin, *Environ. Sci. Technol.* 42 (2008) 8930–8934.
- [15] S.Y. Cheng, D.L. Oatley, P.M. Williams, C.J. Wright, Characterisation and application of a novel positively charged nanofiltration membrane for the treatment of textile industry wastewaters, *Water. Res.* 46 (2012) 33–42.
- [16] C. Ling, F.Q. Liu, C. Long, T.P. Chen, Q.Y. Wu, A.M. Li, Synergic removal and sequential recovery of acid black 1 and copper (II) with hyper-crosslinked resin and inside mechanisms, *Chem. Eng. J.* 236 (2014) 323–331.
- [17] L. Kabalalah-Amitai, B. Mayzel, P. Zaslansky, Y. Kauffmann, P. Clotens, B. Pokroy, Unique crystallographic pattern in the macro to atomic structure of *Herdmania momus* vaterite spicules, *J. Struct. Biol.* 183 (2013) 191–198.
- [18] L. Kabalalah-Amitai, B. Mayzel, Y. Kauffmann, A.N. Fitch, L. Bloch, P.U.P.A. Gilbert, B. Pokroy, Vaterite crystals contain two interspersed crystal structures, *Science* 340 (2013) 454–457.
- [19] G.T. Zhou, J.C. Yu, X.C. Wang, L.Z. Zhang, Sonochemical synthesis of aragonite-type calcium carbonate with different morphologies, *New J. Chem.* 28 (2004) 1027–1031.
- [20] W. Johannes, D. Puhan, Calcite-aragonite transition, reinvestigated, *Mineral. Petrol.* 31 (1971) 28–38.
- [21] E. Griesshaber, K. Kelm, A. Sehrbrock, W. Mader, J. Mutterlose, U. Brand, W.W. Schmahl, Amorphous calcium carbonate in the shell material of the brachiopod *Megerlia truncata*, *Eur. J. Mineral.* 21 (2009) 715–723.
- [22] Y.S. Han, G. Hadiko, M. Fujii, M. Takahashi, A novel approach to synthesize hollow calcium carbonate particles, *Chem. Lett.* 34 (2005) 152–153.
- [23] S.J. Kohler, P. Cubillas, J.D. Rodriguez-Blanco, C. Bauer, M. Prieto, Removal of cadmium from wastewaters by aragonite shells and the influence of other divalent cations, *Environ. Sci. Technol.* 41 (2007) 112–118.
- [24] H. Merrikhpour, M. Jalali, Waste calcite sludge as an adsorbent for the removal of cadmium, copper, lead, and zinc from aqueous solutions, *Clean Technol. Environ. Policy* 14 (2012) 845–855.
- [25] O. Yavuz, R. Guzel, F. Aydin, I. Tegin, R. Ziyadanogullari, Removal of cadmium and lead from aqueous solution by calcite, *Pol. J. Environ. Stud.* 16 (2007) 467–471.
- [26] G.B. Cai, G.X. Zhao, X.K. Wang, S.H. Yu, Synthesis of polyacrylic acid stabilized amorphous calcium carbonate nanoparticles and their application for removal of toxic heavy metal ions in water, *J. Phys. Chem. C* 114 (2010) 12948–12954.
- [27] Y. Du, F. Lian, L.Y. Zhu, Biosorption of divalent Pb, Cd and Zn on aragonite and calcite mollusk shells, *Environ. Pollut.* 159 (2011) 1763–1768.
- [28] X.M. Ma, L.P. Li, L. Yang, C.Y. Su, K. Wang, K. Jiang, Preparation of hybrid CaCO₃-pepsin hemisphere with ordered hierarchical structure and the application for removal of heavy metal ions, *J. Cryst. Growth* 338 (2012) 272–279.
- [29] Y. Du, L.Y. Zhu, G.Q. Shan, Removal of Cd²⁺ from contaminated water by nano-sized aragonite mollusk shell and the competition of coexisting metal ions, *J. Colloid Interface Sci.* 367 (2012) 378–382.
- [30] A.M. Lopez-Marzo, J. Pons, A. Merkoci, Extremely fast and high Pb²⁺ removal capacity using a nanostructured hybrid material, *J. Mater. Chem. A* 2 (2014) 8766–8772.
- [31] J. Zhang, B. Yao, H. Ping, Z.Y. Fu, Y. Li, W.M. Wang, H. Wang, Y.C. Wang, J.Y. Zhang, F. Zhang, Template-free synthesis of hierarchical porous calcium carbonate microspheres for efficient water treatment, *Rsc. Adv.* 6 (2016) 472–480.
- [32] J. Saikia, B. Saha, G. Das, Morphosynthesis of framboidal stable vaterite using a salicylic acid-aniline dye as an additive, *Rsc. Adv.* 2 (2012) 10015–10019.
- [33] M. Kitamura, Crystallization and transformation mechanism of calcium carbonate polymorphs and the effect of magnesium ion, *J. Colloid Interface Sci.* 236 (2001) 318–327.
- [34] A. Godelitsas, J.M. Astilleros, Dissolution, sorption/(re)precipitation, formation of solid solutions and crystal growth phenomena on mineral surfaces: implications for the removal of toxic metals from the environment, in: M. Prieto, H. Stoll (Eds.), *Ion Partitioning in Ambient-Temperature Aqueous Systems*, EMU Notes in Mineralogy, 10, European Mineralogical Union and the Mineralogical Society of Great Britain & Ireland, London, 2010, pp. 289–324.
- [35] L. Long, Y.W. Xue, Y.F. Zeng, K. Yang, C.J. Lin, Synthesis, characterization and mechanism analysis of modified crayfish shell biochar possessed ZnO nanoparticles to remove trichloroacetic acid, *J. Clean. Prod.* 166 (2017) 1244–1252.
- [36] M. Prieto, P. Cubillas, Á. Fernández-Gonzalez, Uptake of dissolved Cd by biogenic and abiogenic aragonite: a comparison with sorption onto calcite, *Geochim. Cosmochim. Acta* 67 (2003) 3859–3869.
- [37] X.M. Ma, S.B. Yuan, L. Yang, L.P. Li, X.T. Zhang, C.Y. Su, K. Wang, Fabrication and potential applications of CaCO₃-lentinan hybrid materials with hierarchical composite pore structure obtained by self-assembly of nanoparticles, *CrystEngComm* 15 (2013) 8288–8299.
- [38] R.S. Lokhande, P.U. Singare, D.S. Pimple, Toxicity study of heavy metals pollutants in waste water effluent samples collected from Talaja Industrial Estate of Mumbai, India, *Res. Environ* 1 (2011) 13–19.
- [39] G.T. Zhou, Q.Z. Yao, S.Q. Fu, Y.B. Guan, Controlled crystallization of unstable vaterite with distinct morphologies and their polymorphic transition to stable calcite, *Eur. J. Mineral.* 22 (2010) 259–269.
- [40] Q.J. Xiang, B. Cheng, J.G. Yu, Hierarchical porous CdS nanosheet-assembled flowers with enhanced visible-light photocatalytic H₂-production performance, *Appl. Catal., B* 138 (2013) 299–303.
- [41] Y.Y. Wang, Q.Z. Yao, H. Li, G.-T. Zhou, Y.-M. Sheng, Formation of vaterite mesocrystals in biomineral-like structures and implication for biomineralization, *Cryst. Growth Des* 15 (2015) 1714–1725.
- [42] Y. Levi, S. Albeck, A. Brack, S. Weiner, L. Addadi, Control over aragonite crystal nucleation and growth: An in vitro study of biomineralization, *Chem. - Eur. J.* 4 (1998) 389–396.
- [43] O. Abollino, M. Aceto, M. Malandrino, C. Sarzanini, E. Mentasti, Adsorption of heavy metals on Na-montmorillonite. Effect of pH and organic substances, *Water. Res.* 37 (2003) 1619–1627.
- [44] Y.X. Huang, A.A. Keller, EDTA functionalized magnetic nanoparticle sorbents for cadmium and lead contaminated water treatment, *Water. Res.* 80 (2015) 159–168.
- [45] Z.L. Du, T. Zheng, P. Wang, L.L. Hao, Y.X. Wang, Fast microwave-assisted preparation of a low-cost and recyclable carboxyl modified lignocellulose-biomass jute fiber for enhanced heavy metal removal from water, *Bioresour. Technol* 201 (2016) 41–49.
- [46] R. Karthik, S. Meenakshi, Removal of Pb(II) and Cd(II) ions from aqueous solution using polyaniline grafted chitosan, *Chem. Eng. J.* 263 (2015) 168–177.
- [47] X.M. Ma, L.P. Li, L. Yang, C.Y. Su, K. Wang, S.B. Yuan, J.G. Zhou, Adsorption of heavy metal ions using hierarchical CaCO₃-maltose meso/macroporous hybrid materials: adsorption isotherms and kinetic studies, *J. Hazard. Mater.* 209 (2012) 467–477.
- [48] P. Cubillas, S. Köhler, M. Prieto, C. Causerand, E.H. Oelkers, How do mineral coatings affect dissolution rates? An experimental study of coupled CaCO₃ dissolution-CdCO₃ precipitation, *Geochim. Cosmochim. Acta* 69 (2005) 5459–5476.
- [49] N. Vdovic, D. Kralj, Electrokinetic properties of spontaneously precipitated calcium carbonate polymorphs: the influence of organic substances, *Colloids Surf., A* 161 (2000) 499–505.
- [50] M.C.S. Reddy, L. Sivaramakrishna, A.V. Reddy, The use of an agricultural waste material, Jujuba seeds for the removal of anionic dye (Congo red) from aqueous medium, *J. Hazard. Mater.* 203 (2012) 118–127.
- [51] Y.J. Yao, S.D. Miao, S.Z. Liu, L.P. Ma, H.Q. Sun, S.B. Wang, Synthesis, characterization, and adsorption properties of magnetic Fe₃O₄@graphene nanocomposite, *Chem. Eng. J.* 184 (2012) 326–332.
- [52] P.Y. Wang, X.X. Wang, S.J. Yu, Y.D. Zou, J. Wang, Z.S. Chen, N.S. Alharbi, A. Alsaedi, T. Hayat, Y.T. Chen, X.K. Wang, Silica coated Fe₃O₄ magnetic nanospheres for high removal of organic pollutants from wastewater, *Chem. Eng. J.* 306 (2016) 280–288.
- [53] M.O. Ansari, R. Kumar, S.A. Ansari, S.P. Ansari, M.A. Barakat, A. Alshahrie, M.H. Cho, Anion selective pTSA doped polyaniline/graphene oxide-multiwalled carbon nanotube composite for Cr(VI) and Congo red adsorption, *J. Colloid Interface Sci.* 496 (2017) 407–415.
- [54] W.Z. Yin, S. Hao, H.Q. Cao, Solvothermal synthesis of magnetic CoFe₂O₄/rGO nanocomposites for highly efficient dye removal in wastewater, *Rsc. Adv.* 7 (2017) 4062–4069.
- [55] G.T. Zhou, Y.F. Zheng, Chemical synthesis of CaCO₃ minerals at low temperatures and implication for mechanism of polymorphic transition, *N. Jb. Mineral. Abh.* 176 (2001) 323–343.
- [56] L. Wang, A.Q. Wang, Adsorption properties of Congo Red from aqueous solution onto surfactant-modified montmorillonite, *J. Hazard. Mater.* 160 (2008) 173–180.

- [57] L.X. Wang, J.C. Li, Z.T. Wang, L.J. Zhao, Q. Jiang, Low-temperature hydrothermal synthesis of alpha-Fe/Fe₃O₄ nanocomposite for fast Congo red removal, *Dalton Trans.* 42 (2013) 2572–2579.
- [58] A.T. Nagaraja, S. Pradhan, M.J. McShane, Poly (vinylsulfonic acid) assisted synthesis of aqueous solution stable vaterite calcium carbonate nanoparticles, *J. Colloid Interface Sci.* 418 (2014) 366–372.
- [59] H.X. Guo, P.Z. Sun, Z.P. Qiu, L.L. Shan, G.J. Zhang, S.P. Cui, Y.C. Liang, Sodium lignosulfonate induced vaterite calcium carbonate with multilayered structure, *Eur. J. Inorg. Chem.* 2014 (2014) 1001–1009.
- [60] F. Manoli, E. Dalas, Spontaneous precipitation of calcium carbonate in the presence of chondroitin sulfate, *J. Cryst. Growth* 217 (2000) 416–421.
- [61] D.H. Chu, M. Vinoba, M. Bhagiyalakshmi, I.H. Baek, S.C. Nam, Y. Yoon, S.H. Kim, S.K. Jeong, CO₂ mineralization into different polymorphs of CaCO₃ using an aqueous-CO₂ system, *Rsc. Adv.* 3 (2013) 21722–21729.
- [62] P. Huang, X. Zhang, J.M. Wei, J.Q. Pan, Y.Z. Sheng, B.X. Feng, The preparation, characterization and optical properties of Cd₂V₂O₇ and CdCO₃ compounds, *Mater. Chem. Phys.* 147 (2014) 996–1002.
- [63] G. Jalani, M. Cerruti, Nano graphene oxide-wrapped gold nanostars as ultrasensitive and stable SERS nanoprobe, *Nanoscale* 7 (2015) 9990–9997.
- [64] S.B. Hartono, S.Z. Qiao, K. Jack, B.P. Ladewig, Z.P. Hao, G.Q. Lu, Improving adsorbent properties of cage-like ordered amine functionalized mesoporous silica with very large pores for bioadsorption, *Langmuir* 25 (2009) 6413–6424.
- [65] T.P. Chen, F.Q. Liu, C. Ling, J. Gao, C. Xu, L.J. Li, A.M. Li, Insight into highly efficient core-removal of copper and p-nitrophenol by a newly synthesized polyamine chelating resin from aqueous media: competition and enhancement effect upon site recognition, *Environ. Sci. Technol.* 47 (2013) 13652–13660.
- [66] C.K. Liu, R.B. Bai, Q.S. Ly, Selective removal of copper and lead ions by diethylenetriamine-functionalized adsorbent: behaviors and mechanisms, *Water Res.* 42 (2008) 1511–1522.
- [67] C. Ling, F.Q. Liu, C. Xu, T.P. Chen, A.M. Li, An integrative technique based on synergistic core-removal and sequential recovery of copper and tetracycline with dual-functional chelating resin: roles of amine and carboxyl groups, *ACS Appl. Mater. Interfaces* 5 (2013) 11808–11817.